

MATHEMATICAL MODELLING AND ANALYSIS
VOLUME 9 NUMBER 1, 2004, PAGES 51–66
© 2004 Technika ISSN 1392-6292

DYNAMICS OF MULTISECTION SEMICONDUCTOR LASERS

J. SIEBER¹, M. RADŽIŪNAS² and K. R. SCHNEIDER²

¹ *University of Bristol*

Dept. of Eng. Math., Queen's Building, University of Bristol, Bristol BS8 1TR,
United Kingdom

E-mail: jan.sieber@bristol.ac.uk

² *Weierstrass Institute for Applied Analysis and Stochastics, Berlin*

Mohrenstr. 39, 10117 Berlin, Germany

E-mail: radziunas@wias-berlin.de; schneider@wias-berlin.de

Received October 10 2003; revised December 19 2003

Abstract. We investigate the longitudinal dynamics of multisection semiconductor lasers based on a model, where a hyperbolic system of partial differential equations is nonlinearly coupled with a system of ordinary differential equations. We present analytic results for that system: global existence and uniqueness of the initial-boundary value problem, and existence of attracting invariant manifolds of low dimension. The flow on these manifolds is approximately described by the so-called mode approximations which are systems of ordinary differential equations. Finally, we present a detailed numerical bifurcation analysis of the two-mode approximation system and compare it with the simulated dynamics of the full PDE model.

Key words: laser dynamics, invariant manifold theory, hyperbolic systems of partial differential equations, model reduction, bifurcation analysis

1. Motivation

In commercial and public communication, the exchange of multimedial information growths rapidly. Thus, the corresponding data traffic increases exponentially and is characterized by the shift from voice communication to package oriented data traffic. This fact implies a big challenge for a strong increase of the data transmission rate. Due to their inherent speed, semiconductor lasers are of great interest as optical devices for fast data regeneration (reamplification, retiming, reshaping) in future photonic networks. Typically, these devices have a non-stationary working regime. As an example we mention the regime of high-frequency oscillations. Multisection lasers allow one to generate and to control such nonlinear effects by designing the longitudinal structure of the device (see, e.g., [16, 19, 25, 28]).

However, prototyping of multisection semiconductor lasers is very expensive and time consuming. The goal of this paper is to demonstrate that mathematical models can be used to study the longitudinal dynamics of such lasers and to optimize their working regime.

We focus on the traveling wave model, a linear hyperbolic system of partial differential equations (PDEs) which is nonlinearly coupled with a system of ordinary differential equations (ODEs). It models the longitudinal dynamics of edge emitting multisection semiconductor lasers by the interaction of two physical variables: the complex light amplitude (in fact, its spatially slowly varying envelope), which is spatially resolved in the longitudinal direction of the laser and described by the linear hyperbolic PDE subsystem, and the effective carrier density within the active zone of the device, which is section-wise spatially averaged and described by the ODE subsystem.

This model has the advantage of meeting two seemingly contradictory criteria, accuracy and simplicity (or rather accessibility to a detailed bifurcation analysis). On one hand, it is accurate enough to describe all phenomena of interest to the engineers. Moreover, it can easily be made more realistic by gradually incorporating secondary physical effects that may play a role in limiting the performance of a particular device. On the other hand, it allows one to reduce the model to a low-dimensional system of ODEs by exploiting the fact that the carrier density operates on a much slower time-scale than the light amplitude. These ODEs in turn are accessible to a detailed bifurcation analysis using standard software like AUTO [10]. Only this bifurcation analysis gives insight into the mechanisms behind many nonlinear phenomena and is able to reveal effects (for example excitability [27]) that may be invisible in pure parameter studies.

Both aspects of the traveling wave model have been implemented in the numerical code LDSL (Longitudinal Dynamics of Semiconductor Lasers). Hence, this numerical tool provides engineers, laser physicists, and mathematicians with a whole hierarchy of models allowing them to “switch on or off” physical effects to gain insight which of these effects causes the particular phenomenon they are interested in. Besides numerical integration of the model equations this tool solves also the spectral problem of the model equations, allows to analyze the dynamics of individual longitudinal modes and in certain cases enables one effectively to compare the solutions provided by the PDE model and the reduced mode approximation systems. This modeling approach has been used quite successfully in the recent past to design new devices exhibiting high-frequency oscillations [7, 8, 28].

In this paper we focus more on the aspect of model reduction than extension, mostly because this part is more thoroughly supported by mathematical theory. The paper is organized as follows: In section 2. we describe the traveling wave model and give a detailed physical interpretation of all coefficients and variables. In section 3. we show that the corresponding initial-boundary value problem is well-posed. In section 4. we introduce a small parameter exploiting the difference in the time-scale between light and carrier density. In section 5. we investigate the spectral properties of the infinite-dimensional linear part. Section 6. combines the results of the previous sections to derive conditions guaranteeing that the traveling wave model can be reduced to an ODE system. In section 7. by showing a detailed two-parameter bifur-

cation diagram we demonstrate how useful the reduced model can be. We link this bifurcation diagram to a parameter study with a more realistic version of the traveling wave model. In the last section we draw conclusions and give an outlook on future projects.

2. The coupled traveling wave model with nonlinear gain dispersion

The *coupled traveling wave model*, a hyperbolic system of PDEs coupled with a system of ODEs, describes the longitudinal effects in narrow edge-emitting laser diodes [1, 15, 23]. It has been derived from Maxwell's equations for an electro-magnetic field in a periodically modulated waveguide [1, 3] assuming that transversal and longitudinal effects can be separated. In this section we introduce the corresponding

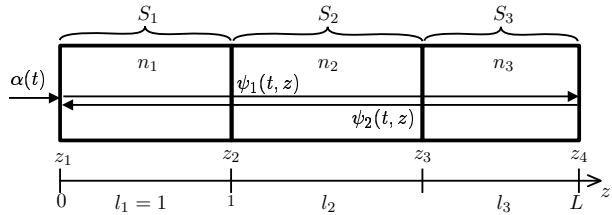


Figure 1. Typical geometric configuration of the domain in a laser with 3 sections.

system of differential equations, explain the physical interpretation of its coefficients and specify some physically sensible assumptions about these coefficients.

The dynamics in a multi-section laser is described by the evolution of the following quantities. The variable $\psi(t, z) \in \mathbb{C}^2$ describes the complex amplitude of the slowly varying envelope of the optical field split into a forward and a backward traveling wave. The variable $p(t, z) \in \mathbb{C}^2$ describes the corresponding nonlinear polarization of the material. Both quantities depend on time and the one-dimensional spatial variable $z \in [0, L]$ (the longitudinal direction within the laser; see Fig. 1). A prominent feature of multi-section lasers is the splitting of the overall interval $[0, L]$ into sections, that is, m subintervals S_k that represent sections with separate electric contacts. We treat the carrier density within the active zone of the waveguide as a section-wise spatially averaged quantity $n(t) \in \mathbb{R}^m$ (see Fig. 1). In dimensionless form, the coupled traveling wave model can be posed as an initial-boundary value problem for ψ , p , and n that reads as follows

$$\partial_t \psi(t, z) = \begin{bmatrix} -\partial_z + \beta(n(t), z) & -i\kappa(z) \\ -i\kappa(z) & \partial_z + \beta(n(t), z) \end{bmatrix} \psi(t, z) + \rho(n(t), z) p(t, z), \quad (2.1)$$

$$\partial_t p(t, z) = [i\Omega_r(n(t), z) - \Gamma(n(t), z)] p(t, z) + \Gamma(n(t), z) \psi(t, z), \quad (2.2)$$

$$\begin{aligned} \frac{d}{dt} n_k(t) &= I_k - \frac{n_k(t)}{\tau_k} - \frac{P}{l_k} [G_k(n_k(t)) - \rho_k(n_k(t))] \int_{S_k} \psi(t, z)^* \psi(t, z) dz \\ &\quad - \frac{P}{l_k} \rho_k(n_k(t)) \operatorname{Re} \left(\int_{S_k} \psi(t, z)^* p(t, z) dz \right), \quad k = 1, \dots, m \end{aligned} \quad (2.3)$$

subject to the inhomogeneous boundary conditions for ψ

$$\psi_1(t, 0) = r_0 \psi_2(t, 0) + \alpha(t), \quad \psi_2(t, L) = r_L \psi_1(t, L) \quad (2.4)$$

and the initial conditions

$$\psi(0, z) = \psi^0(z), \quad p(0, z) = p^0(z), \quad n(0) = n^0. \quad (2.5)$$

The Hermitian transpose of the \mathbb{C}^2 -vector ψ is denoted by ψ^* in (2.3). We will define the appropriate function spaces and discuss the possible solution concepts in section 3.. The quantities and coefficients appearing above have the following meaning (see also Tab. 1 and Fig. 1). L is the length of the laser. The laser is subdivided into

Table 1. Ranges and explanations of the variables and coefficients appearing in (2.1) – (2.4). See also [3] to inspect their relations to the originally used physical quantities and scales.

	typical range	explanation
$\psi(t, z)$	\mathbb{C}^2	optical field, forward and backward traveling wave
$p(t, z)$	\mathbb{C}^2	nonlinear polarization
$n_k(t)$	\mathbb{R}_+	spatially averaged carrier density in section S_k
$\operatorname{Im} d_k$	\mathbb{R}	frequency detuning
$\operatorname{Re} d_k$	$< 0, O(1)$	negative decay rate due to internal losses
$\alpha_{H,k}$	$(0, 10)$	negative of line-width enhancement factor
\tilde{g}_k	≈ 1	differential gain in active sections S_k
κ_k	$(-10, 10)$	real coupling coefficient for the optical field ψ due to Bragg grating in DFB sections
ρ_k	$\geq 0, O(1)$	amplitude of the gain curve
Γ_k	$O(10^2)$	half width at half maximum of the gain curve
$\Omega_{r,k}$	$O(10)$	central frequency of the gain curve
I_k	$O(10^{-2})$	current injection
τ_k	$O(10^2)$	spontaneous lifetime of the carriers
P	$(0, \infty)$	scale of (ψ, p) (can be chosen arbitrarily)
r_0, r_L	$\mathbb{C}, r_0 , r_L < 1$	facet reflectivities

m sections S_k of length l_k with starting points z_k for $k = 1, \dots, m$. We scale the system such that $l_1 = 1$ and set $z_{m+1} = L$. Thus, $S_k = [z_k, z_{k+1}]$. All coefficients are supposed to be spatially constant in each section and to depend only on the carrier density in that section, that is, for $z \in S_k$ we have

$$\kappa(z) = \kappa_k, \quad \Gamma(n, z) = \Gamma_k(n_k), \quad \beta(n, z) = \beta_k(n_k), \quad \rho(n, z) = \rho_k(n_k).$$

Tab. 1 collects the physical interpretation and the sensible ranges of all coefficients and variables. The model for the growth coefficient $\beta_k(n_k) \in \mathbb{C}$ in section S_k is

$$\beta_k(\nu) = d_k + (1 + i\alpha_{H,k})G_k(\nu) - \rho_k(\nu),$$

where $d_k \in \mathbb{C}$ accounts for the static internal losses (hence, $\operatorname{Re} d_k < 0$) and the static frequency detuning, and $\alpha_{H,k} \in \mathbb{R}_+$ is the negative of the line-width enhancement (or Henry) factor. A section S_k is either *passive*, then the functions G_k and ρ_k are identically zero, or S_k is *active*. In the active case $G_k : \mathbb{R} \rightarrow \mathbb{R}$ is a smooth strictly monotone increasing function satisfying $G_k(1) = 0$. Its limits are

$$\lim_{\nu \rightarrow -\infty} G_k(\nu) = -\infty, \quad \lim_{\nu \rightarrow \infty} G_k(\nu) = \infty.$$

Typically, an affine model for G_k in active sections is reasonably accurate, that is,

$$G_k(\nu) = \tilde{g}_k \cdot (\nu - 1)$$

with a differential gain $\tilde{g}_k = G'_k(1) > 0$. In active sections S_k , that is, if $G_k \not\equiv 0$, the gain amplitude $\rho_k(\nu)$ is bounded for $\nu < 1$. Moreover, we suppose that ρ_k , $\Omega_{r,k}$, and $\Gamma_k : \mathbb{R} \rightarrow \mathbb{R}$ are smooth and Lipschitz continuous, and $\Gamma_k(\nu) > 1$ for all ν . For passive sections S_k the variable n_k is decoupled from all other equations and can be dropped from the system.

The polarization function p and equation (2.2) has been included into the coupled traveling wave model for a more realistic account of nonlinear gain dispersion effects [3, 28]. Now, the frequency dependence of waveguide material gain is modeled by a Lorentzian function with an amplitude ρ , half width at half maximum Γ , centered at the frequency Ω_r . That is, a monochromatic light-wave $\psi_1(t, z) = e^{i\omega t} \varphi(z)$ in an uncoupled stationary waveguide ($\kappa = 0$, $\dot{n} = 0$) is amplified or damped according to the equation

$$\partial_z |\varphi(z)|^2 = 2 \left[\operatorname{Re} \beta(z) + \frac{\rho(z)\Gamma^2(z)}{(\omega - \Omega_r(z))^2 + \Gamma^2(z)} \right] |\varphi(z)|^2.$$

The facet reflectivities r_0 and r_L in (2.4) are complex with modulus less than 1. The inhomogeneity $\alpha(t)$ is complex. It models an optical input at the facet $z = 0$. We assume it to be \mathbb{L}^2 in time on finite time intervals to permit a discontinuous optical input.

The form of the right-hand-side of equation (2.3) for the carrier density can be clarified by introducing the Hermitian form

$$g_k(\nu) \begin{bmatrix} (\psi) \\ p \end{bmatrix}, \begin{pmatrix} \varphi \\ q \end{pmatrix} \Big] = \frac{1}{l_k} \int_{S_k} (\psi^*(z), p^*(z)) \begin{pmatrix} G_k(\nu) - \rho_k(\nu) & \frac{1}{2}\rho_k(\nu) \\ \frac{1}{2}\rho_k(\nu) & 0 \end{pmatrix} \begin{pmatrix} \varphi(z) \\ q(z) \end{pmatrix} dz.$$

Using the notation

$$f_k(\nu, (\psi, p)) = I_k - \frac{\nu}{\tau_k} - P g_k(\nu) \begin{bmatrix} (\psi) \\ p \end{bmatrix} \quad (2.6)$$

for $\nu \in \mathbb{R}$ and $\psi, \varphi, p, q \in \mathbb{L}^2(S_k; \mathbb{C}^2)$ the carrier density equation (2.3) reads

$$\frac{d}{dt}n_k = f_k(n_k, (\psi, p)) \quad \text{for } k = 1, \dots, m. \quad (2.7)$$

Other secondary physical effects have been incorporated into the numerical code LDSL which was developed for the simulation and analysis of longitudinal dynamics in multi-section lasers. As example we mention the effects of nonlinear gain compression, that is, the dependence of G on $|\psi|^2$, and spatial hole burning, i.e., treating n as a fully spatially resolved variable [7, 28]. The parameter study by direct simulations of the extended model equations shown in Fig. 3 has taken both effects into account. However, even after an inclusion of these effects, the traveling wave model can describe the behaviour of semiconductor lasers still only approximately. Thus, in this paper we focus on the analysis of the traveling wave model in the rather simple form (2.1) – (2.4).

3. Existence theory

In a first step we investigate in which sense system (2.1) – (2.3) generates a semiflow depending smoothly on its initial values and all parameters. We want to write (2.1) – (2.3) as an abstract evolution equation in the form

$$\frac{d}{dt}u = Au + g(u), \quad u(0) = u_0 \quad (3.1)$$

in a Hilbert space V , where A is a linear differential operator that generates a strongly continuous semigroup $S(t)$, and g is smooth in V . A natural space for the variables ψ and p is $\mathbb{L}^2([0, L]; \mathbb{C}^2)$, such that V could be $\mathbb{L}^2([0, L]; \mathbb{C}^2) \times \mathbb{L}^2([0, L]; \mathbb{C}^2) \times \mathbb{R}^m$ for $u = (\psi, p, n)$. However, the inhomogeneity α in the boundary condition (2.4) poses a conceptual difficulty in this framework. Common approaches are boundary homogenization (used in [18]) or appending α as an auxiliary variable and an additional equation of the form

$$\frac{d}{dt}\alpha(t) = a(t),$$

where a is the derivative of α (used in [12]). Then, the nonlinearity g in the evolution equation depends explicitly on t and it has the same regularity with respect to t as the time derivative of α . Hence, both approaches require a high degree of regularity of α in time which is quite unnatural as the laser still works with discontinuous input such as square waves. An alternative would be the introduction of a concept of “weakly mild” solutions as it was done in [13]. However, this would require the extension of all needed classical results of the theory of strongly continuous semigroups to this type of solutions.

Here, we choose an approach that is similar to that in [12] but does not require any regularity of the inhomogeneity. We introduce the auxiliary space-dependent variable $a(t, x)$ ($x \in [0, \infty)$) satisfying the equation

$$\partial_t a(t, x) = \partial_x a(t, x) \quad (3.2)$$

and change the boundary condition for $z = 0$ in (2.4) into

$$\psi_1(t, 0) = r_0\psi_2(t, 0) + a(t, 0).$$

One may think of an infinitely long fibre $[0, \infty)$ storing all future optical inputs and transporting them to the laser facet $z = x = 0$ by the transport equation (3.2). If we choose $a(0, x) = \alpha(x)$ as initial value for a , than the value of a at the boundary $x = 0$ at time t is $\alpha(t)$. In this way, the initially inhomogeneous boundary condition becomes linear in the variables ψ and a requiring no regularity for a . We choose a weighted norm \mathbb{L}_η^2 for a , that is, $\|a(t, \cdot)\|^2 = \int_0^\infty |a(t, x)|^2(1 + x^2)^\eta dx$ with $\eta < -1/2$. In this way, we permit the input to be \mathbb{L}^∞ but still keep V as a Hilbert space.

With this modification we can work within the framework of the theory of strongly continuous semigroups [17]. The variable u has the components $(\psi, p, n, a) \in V = \mathbb{L}^2([0, L]; \mathbb{C}^2) \times \mathbb{L}^2([0, L]; \mathbb{C}^2) \times \mathbb{R}^m \times \mathbb{L}_\eta^2([0, \infty); \mathbb{C})$. We have a certain freedom how to choose the splitting of the right-hand-side between A and g . We keep A as simple as possible, including only the unbounded terms

$$A \begin{bmatrix} \psi \\ p \\ n \\ a \end{bmatrix} := \begin{bmatrix} -\partial_z \psi_1 \\ \partial_z \psi_2 \\ 0 \\ 0 \\ \partial_x a \end{bmatrix}.$$

The domain of definition of A is

$$D(A) = \{(\psi, p, n, a) \in \mathbb{H}^1([0, L]; \mathbb{C}^2) \times \mathbb{L}^2([0, L]; \mathbb{C}^2) \times \mathbb{R}^m \times \mathbb{H}_\eta^1([0, \infty); \mathbb{C}) : \psi_1(0) = r_0\psi_2(0) + a(0), \psi_2(L) = r_L\psi_1(L)\}.$$

In this way, A generates a strongly continuous semigroup $S(t)$ in V [22]. The non-linearity g is smooth because it is a superposition operator of smooth coefficient functions, and all components either depend only linearly on the infinite-dimensional components ψ and p , or map into \mathbb{R}^m . Then, an a-priori estimate implies the following theorem.

Theorem 1 [Global existence and uniqueness]. *For any $T_0 > 0$, there exists a unique mild solution $u(t)$ of (3.1) in $[0, T_0]$. Furthermore, if the initial value u_0 is in the domain of definition of A , then $u(t)$ is a classical solution of (3.1).*

This theorem implies the existence of a semiflow $S(t; u_0)$ that is strongly continuous in t and smooth with respect to u and parameters. The a-priori estimate has to be slightly more subtle than in [18]. It uses the fact that the same functions G_k and ρ_k appear on the right-hand-side of (2.1) and on that of (2.3) but with opposing signs. Due to this fact the function

$$\frac{P}{2} \|\psi(t)\|^2 + \sum_{k=1}^m l_k(n_k(t) - n_*)$$

remains non-negative for sufficiently small n_* and, hence, bounded, giving rise to a bounded invariant ball in V . The value of n_* depends on the initial value u_0 (see [22] for details).

4. Introduction of a small parameter

For all results about the long-time behavior of system (2.1) – (2.3) we restrict ourselves to autonomous boundary conditions for ψ , that is,

$$\psi_1(t, 0) = r_0 \psi_2(t, 0), \quad \psi_2(t, L) = r_L \psi_1(t, L). \quad (4.1)$$

The inhomogeneous case is an open question for future work. However, understanding the dynamics of the autonomous laser is not only an intermediate step but an important goal in itself since many experiments and simulations focus on this case; see for example [8] for further references.

An examination of system (2.1) – (2.3) reveals that the space dependent subsystem is linear in ψ and p :

$$\partial_t \begin{pmatrix} \psi \\ p \end{pmatrix} = H(n) \begin{pmatrix} \psi \\ p \end{pmatrix}. \quad (4.2)$$

The linear operator

$$H(n) = \begin{pmatrix} \begin{bmatrix} -\partial_z + \beta(n) & -i\kappa \\ -i\kappa & \partial_z + \beta(n) \end{bmatrix} & \rho(n) \\ \Gamma(n) & i\Omega_r(n) - \Gamma(n) \end{pmatrix} \quad (4.3)$$

acts from

$$\begin{aligned} Y := \{(\psi, p) \in \mathbb{H}^1([0, L]; \mathbb{C}^2) \times \mathbb{L}^2([0, L]; \mathbb{C}^2) : \\ \psi_1(0) = r_0 \psi_2(0), \quad \psi_2(L) = r_L \psi_1(L)\} \end{aligned}$$

into $X = \mathbb{L}^2([0, L]; \mathbb{C}^2) \times \mathbb{L}^2([0, L]; \mathbb{C}^2)$. $H(n)$ generates a C_0 -semigroup $T_n(t)$ acting in X . Its coefficients κ , and, for each $n \in \mathbb{R}^m$, $\beta(n)$, $\Omega_r(n)$, $\Gamma(n)$ and $\rho(n)$ are linear operators in $\mathbb{L}^2([0, L]; \mathbb{C}^2)$ defined by the corresponding coefficients in (2.1), (2.2). The maps $\beta, \rho, \Gamma, \Omega_r : \mathbb{R}^m \rightarrow \mathcal{L}(\mathbb{L}^2([0, L]; \mathbb{C}^2))$ are smooth.

Furthermore, we observe that I_k and τ_k^{-1} in (2.6) are approximately two orders of magnitude smaller than 1 (see Tab. 1). Hence, we can introduce a small parameter ε and set $P = \varepsilon$ in (2.3), such that the carrier density equation (2.7) reads as

$$\frac{d}{dt} n_k = f_k(n_k, E) = \varepsilon(F_k(n_k) - g_k(n_k)[E, E]) \quad (4.4)$$

for $E \in X$, where the coefficients in $F_k(n_k) = \varepsilon^{-1}(I_k - n_k \tau_k^{-1})$ are of order 1. Although ε is not directly accessible, we treat it as a parameter and consider the limit $\varepsilon \rightarrow 0$ while keeping F_k fixed. At $\varepsilon = 0$, the carrier density n is constant. It enters the linear subsystem (4.2) as a parameter. Consequently, the spectral properties of $H(n)$ with fixed n determine the longtime behavior of the system for $\varepsilon = 0$. In particular, we are interested in such values of n which imply an isolated non-empty but finite set of eigenvalues of $H(n)$ located exactly on the imaginary axis. In this case, we can expect a finite-dimensional invariant manifold to persist for nonzero ε in the spirit of Fenichel's geometric singular perturbation theory [11]. Thus, we would like to understand the spectral properties of the operator H for fixed n and their correspondence to the growth of the semigroup T_n generated by H in the next step.

5. Spectral properties of operator H

We drop the argument n in this paragraph for brevity. The long-time behavior of the semigroup T generated by H can be described by the following theorem (see [22] for details of the proof):

Theorem 2. *Let $\xi_0 = \frac{1}{L} \sum_{k=1}^m \operatorname{Re} \beta_k l_k < 0$, denote $\mathcal{W} = \{i\Omega_{r,k} - \Gamma_k : k = 1, \dots, m\}$, and let ξ be in the interval $(\max\{\operatorname{Re} \mathcal{W}, \xi_0\}, 0)$. Then, there exists a splitting of $X = X_1 \oplus X_2$ into two H -invariant subspaces where X_1 is finite-dimensional and the semigroup T restricted to X_2 decays according to rate ξ :*

$$\|T(t)|_{X_2}\| \leq M e^{\xi t} \quad \text{for a constant } M \geq 1 \text{ and all } t \geq 0.$$

Since T is neither an analytical nor an eventually compact semigroup there are no general theorems implying our result. However, the operator H has a characteristic function $h(\lambda)$ defined in $\mathbb{C} \setminus \mathcal{W}$ (note that $\operatorname{Re} \mathcal{W} < -1$). The function h is analytic in $\mathbb{C} \setminus \mathcal{W}$ and known explicitly. Hence, most questions about the spectrum of H can be answered by finding the roots of h . In particular, the spectrum of H is discrete in $\mathbb{C} \setminus \mathcal{W}$, that is, it consists only of eigenvalues of finite algebraic multiplicity. In order to obtain our result, we have to distinguish two cases, $r_0 r_L = 0$ and $r_0 r_L \neq 0$.

It turns out that the semigroup T is eventually differentiable if $r_0 r_L = 0$. In this case, we can split X into two H -invariant subspaces. One corresponds to the spectrum close to \mathcal{W} . Thus, H is bounded and T exponentially decaying in this subspace. The semigroup T restricted to the complementary invariant subspace is eventually compact. Hence, the desired result follows from the theory of eventually compact semigroups [9].

If $r_0 r_L \neq 0$ (the hyperbolic case), we treat the operator as a perturbation of its diagonal part similar to [20]. Before applying the same result as [20], the invariant subspace corresponding to the spectrum close to \mathcal{W} has to be split off and treated separately in the same way as in the case $r_0 r_L = 0$.

In essence, Theorem 2 implies that we can treat H like a matrix: the dominant eigenvalues determine the growth of the corresponding semigroup.

6. Model reduction

Let us assume that there exists a simple connected open set $U \subset \mathbb{R}^m$ of carrier densities n such that $H(n)$ has a uniform spectral gap for all $n \in U$ in a strip of the negative complex half-plane $\{z \in \mathbb{C} : \xi \leq \operatorname{Re} z \leq \xi/k\}$ ($\xi < 0$, integer $k > 2$), and that the dominant part of the spectrum of $H(n)$ is finite. Hence, the spectral projection $P_c(n)$ onto the $H(n)$ -invariant subspace corresponding to the dominant part of the spectrum has a constant rank $q > 0$. This spectral gap assumption is quite natural and follows (in conjunction with Theorem 2) for example from the existence of non-trivial dynamics that is uniformly bounded for $\varepsilon \rightarrow 0$ (e.g., relative equilibria, i.e., solutions of the form $E(t) = E_0 e^{i\omega t}$, $n = \text{const}$) if $r_0 r_L = 0$. We can split any $E \in X$ into $E = B(n)E_c + E_s$, where $B(n)$ is a basis of $\operatorname{Im} P_c(n)$ depending smoothly on n , $E_c \in \mathbb{C}^q$, and $E_s \in X$ is $E - P_c(n)B(n)E_c$. The map $\mathcal{R} : X \times U \rightarrow \mathbb{C}^q \times U$ given by $(E, n) \rightarrow (B(n)^{-1}P_c(n)E, n)$ is well defined,

smooth and Lipschitz continuous on any closed subset of $X \times U$. Then, the main model reduction theorem is as follows.

Theorem 3 [Model reduction]. *Let $\varepsilon_0 > 0$ be sufficiently small, $\Delta \in (\xi, 0)$, and \mathcal{N} be a closed bounded subset of $\mathbb{C}^q \times U$. Then, for all $\varepsilon \in [0, \varepsilon_0)$ there exists a C^k manifold $\mathcal{C} \subset X \times \mathbb{R}^m$ satisfying:*

- i. (Invariance) \mathcal{C} is $S(t, \cdot)$ -invariant relative to $\mathcal{R}^{-1}\mathcal{N}$. That is, if $(E, n) \in \mathcal{C}$, $t \geq 0$, and $S([0, t]; (E, n)) \subset \mathcal{R}^{-1}\mathcal{N}$, then $S([0, t]; (E, n)) \subset \mathcal{C}$.
- ii. (Representation) \mathcal{C} can be represented as the graph of a map which maps

$$(E_c, n, \varepsilon) \in \mathcal{N} \times [0, \varepsilon_0) \rightarrow ([B(n) + \varepsilon\nu(E_c, n, \varepsilon)]E_c, n) \in X \times \mathbb{R}^m,$$

where $\nu : \mathcal{N} \times [0, \varepsilon_0) \rightarrow \mathcal{L}(\mathbb{C}^q; X)$ is C^{k-2} with respect to all arguments. Denote the X -component of \mathcal{C} by

$$E_X(E_c, n, \varepsilon) = [B(n) + \varepsilon\nu(E_c, n, \varepsilon)]E_c \in X.$$

- iii. (Exponential attraction) Let $\Upsilon \subset X \times \mathbb{R}^m$ be a bounded set with $\mathcal{R}\Upsilon \subset \mathcal{N}$ and a positive distance to the boundary of \mathcal{N} . Then, there exist a constant M and a time $t_c \geq 0$ with the following property: For any $(E, n) \in \Upsilon$ there exists a $(E_c, n_c) \in \mathcal{N}$ such that

$$\|S(t + t_c; (E, n)) - S(t; (E_X(E_c, n_c, \varepsilon), n_c))\| \leq M e^{\Delta t}$$

for all $t \geq 0$ with $S([0, t + t_c]; (E, n)) \subset \Upsilon$.

- iv. (Flow) The flow on $\mathcal{C} \cap \mathcal{R}^{-1}\mathcal{N}$ is differentiable with respect to t and governed by the following system of ODEs:

$$\begin{cases} \frac{dE_c}{dt} = [H_c(n) + \varepsilon a_1(E_c, n, \varepsilon) + \varepsilon^2 a_2(E_c, n, \varepsilon)\nu(E_c, n, \varepsilon)] E_c, \\ \frac{dn}{dt} = \varepsilon F(E_c, n, \varepsilon), \end{cases} \quad (6.1)$$

where

$$\begin{aligned} H_c(n) &= B(n)^{-1} H(n) P_c(n) B(n), \\ a_1(E_c, n, \varepsilon) &= -B(n)^{-1} P_c(n) \partial_n B(n) F(E_c, n, \varepsilon), \\ a_2(E_c, n, \varepsilon) &= B(n)^{-1} \partial_n P_c(n) F(E_c, n, \varepsilon) (Id - P_c(n)), \\ F(E_c, n, \varepsilon) &= (F_k(n_k) - g_k(n_k)[E_X(E_c, n_c, \varepsilon), E_X(E_c, n_c, \varepsilon)])_{k=1}^m. \end{aligned}$$

The idea to choose n -dependent coordinates for E in the construction of a reduced model was introduced already in [1] by physicists. This choice has the advantage that the graph of the center manifold itself enters the flow (6.1) on the center manifold only in the form $O(\varepsilon^2)\nu$. This fact has been pointed out first in [24], where the same model reduction result has been proven for ODEs of similar structure (big linear system coupled to a slow system) using Fenichel's theorem for singularly perturbed systems of ODEs [11]. Since Fenichel's theorem is not available for infinite-dimensional systems, we have to adapt the proof of Fenichel [11] to our case starting from the general results in [4, 5, 6] about invariant manifolds of semiflows in Banach

spaces. In particular, we apply the cut-off modifications done in [11] only to the finite-dimensional components E_c and n outside of the set \mathcal{N} of interest. Moreover, we adapt the modifications such that the invariant manifold for $\varepsilon = 0$ is compact without boundary as required by the theorems in [4].

Truncating all terms of order $O(\varepsilon^2)$ in (6.1) gives rise to a system of ODEs in $\mathbb{C}^q \times \mathbb{R}^m$, where all terms in the right-hand-side can be expressed analytically as functions of the eigenvalues of H . The truncated system

$$\begin{cases} \frac{dE_c}{dt} = [H_c(n) + \varepsilon a_1(E_c, n, \varepsilon)] E_c, \\ \frac{dn_k}{dt} = \varepsilon (F_k(n_k) - g_k(n_k)[B(n)E_c, B(n)E_c]) \end{cases} \quad (6.2)$$

is called the *mode approximation*. It is an implicit system of ODEs because the eigenvalues of H are given only implicitly as roots of the characteristic function h of H . The dimension of (6.1) is typically low: q is often either 1 or 2. The consideration of mode approximations has proven to be extremely useful for numerical and analytical investigations of longitudinal effects in multi-section semiconductor lasers; see for example [2, 21, 27] and section 7. for a demonstration.

7. Parameter study and bifurcation analysis for a laser subject to delayed optical feedback

In this section we demonstrate how the traveling wave model helps to detect and understand nonlinear phenomena occurring in multi-section lasers by a bifurcation analysis using the mode approximations and the subsequent systematic parameter study for the full model. We investigate a three-section laser, where S_1 is a single-mode DFB laser (i.e., $\kappa_1 \neq 0, G_1 \neq 0$), S_2 is a passive phase tuning section (i.e., $\kappa_2 = G_2 = \rho_2 = \dot{n}_2 = 0$), and S_3 is an amplifier section (i.e., $\kappa_3 = 0, \rho_3 = 0, G_3 \neq 0$). Since $r_L \neq 0$, this device resembles the classical experiment of a single-mode semiconductor laser which is subject to delayed optical feedback. Section S_1 plays the role of the single-mode laser and the sections S_2 and S_3 form an integrated cavity providing delayed optical feedback from the facet at $z = L$. In this three-section setup the two most important parameters, the feedback strength and the feedback phase $\varphi \sim \text{Im } d_2$ can be tuned continuously in the experiment by changing the currents I_2 and I_3 into the sections S_2 and S_3 (up to feedback strengths close to 1).

Bifurcation analysis.

Since numerical bifurcation analysis tools like AUTO [10] are available for systems of ODEs only, the mode approximations justified in Theorem 3 are extremely helpful.

It turns out that the number q of critical eigenvalues of $H(n)$ is 2 for all relevant carrier densities n . Thus, Theorem 3 applies with $q = 2$ and $m = 2$ (the carrier density n_2 is constant since section S_2 is passive). The center manifold \mathcal{C} has dimension 6 as it is a graph over $\mathbb{C}^2 \times \mathbb{R}^2$. The flow of (6.2) is still symmetric with respect to complex rotation of E_c . Hence, we can reduce it to a 5-dimensional

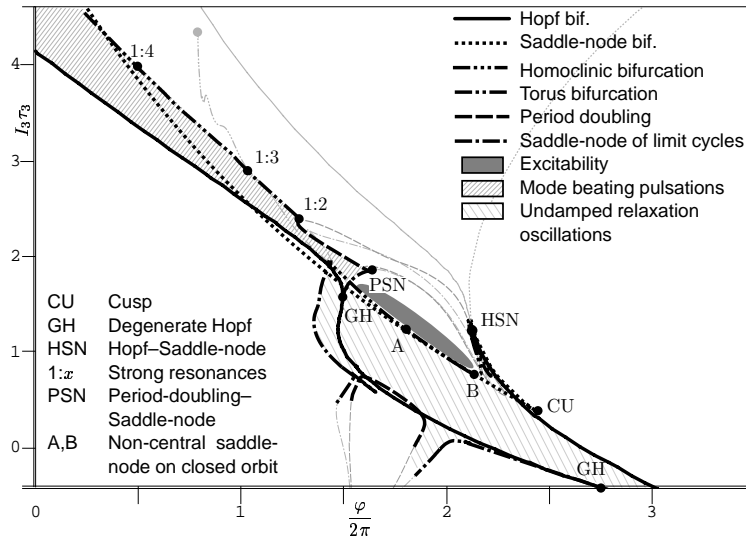


Figure 2. Bifurcation diagram for the two-mode approximation (truncated (6.1) with $q = 2$) in the parameter plane (φ, I_3) (see [7] for the particular parameter values).

system of ODEs. In this system, equilibria correspond to relative equilibria of the original traveling wave model and periodic solutions to self-pulsations, i.e., modulated rotating-wave solutions. Fig. 2 shows the results of two-parameter numerical continuations of the physically most relevant codimension-1 bifurcation curves in the parameter plane (φ, I_3) . The two different islands of self-pulsations are clearly visible along with their borders. The nature of these borders and bifurcation theory serve as a guide for experiment and simulation to investigate interesting phenomena that otherwise could be missed due to hysteresis or limited basins of attraction. Most notably, there are stable invariant tori with strong resonances above the torus bifurcation curve, excitability above the homoclinic bifurcation curve, and period doubling and chaos at the border of the undamped relaxation oscillations.

Parameter study for the full PDE System.

Fig. 3 gives an overview over all stable stationary states and non-stationary regimes that can be found by direct simulation in the parameter plane (φ, I_3) in the full PDE system (2.1) – (2.3). For the simulation, we also included the additional physical effects mentioned at the end of section 2. to match the experimental results as closely as possible. See [7] for a full description of the traveling wave model used in the simulation.

The two large domains of periodic solutions within each period of φ are quite prominent in Fig. 3 as well. The Hopf and the saddle-node curves can be recognized in the simulation and give a full account of the number and stability of all present stationary states in Fig. 3. The shadings in Fig. 3 mark the different stable non-stationary regimes in the (φ, I_3) parameter plane observed in the simulation. Single-pulse periodic solutions are typically born in Hopf bifurcations. Double-pulse

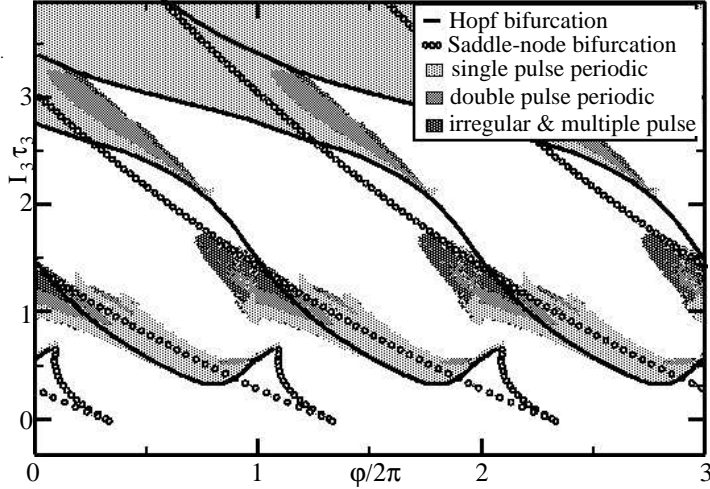


Figure 3. Parameter study of a three section laser by direct simulation of the PDE model with LDSL-tool. Full model and used parameter values (except of $l_1 = 250 \mu\text{m}$, $l_2 = 400 \mu\text{m}$ and $\alpha = 15 \text{ cm}^{-1}$) can be found in [7].

solutions existing nearby have approximately half the frequency. Their occurrence is related to the period doubling bifurcations (see also Fig. 2). Finally, multiple-pulse and irregular regimes account for dynamics (and different resonances) on the tori, and chaotic attractors.

A well-known problem of direct simulations is that only one stable regime will be observed for each parameter value depending on the choice of initial values and the basins of attractions. However, the bifurcation analysis shows that several stable regimes may coexist in some parameter regions. We took into account this possible hysteresis by varying the parameters in small steps in different directions from any stable non-stationary regime we found until we hit a sharp transition. In this way, we always traced the hysteresis at sharp transitions corresponding to subcritical or saddle-node bifurcations. Fig. 3 shows the most simple non-stationary regime in hysteresis parameter regions (that is, mostly, the single-pulse periodic solution) because this is the most interesting regime for potential applications.

8. Conclusions and outlook

The coupled traveling wave model has proven its value in the exploration of nonlinear phenomena in multisection laser structures. This can be seen impressively in recent results concerning delayed optical feedback effects [14, 18, 21, 26, 27], in multi-section lasers and subsequent new device designs [7, 8, 16, 19]. The model has been efficiently implemented in the code LDSL which permits extensive parameter studies. The simulation of the model equations with this code together with the bifurcation analysis of the reduced mode approximation systems gives insight into the underlying dynamics. Moreover, it allows the user to incorporate physical effects

like spatial hole burning or nonlinear gain compression, or experimental conditions like optical input or electric modulation. This broadens the range of applications of the traveling wave model toward mode-locked lasers, optical amplifiers, ring lasers, etc. However, the theory concerning some of these extensions of the traveling wave model is still incomplete, even concerning basic questions like the existence of a smooth strongly continuous semiflow. Thus, an urgent task is to gain a theoretical understanding of these more complex models, and whether they can exhibit substantially more complex phenomena.

References

- [1] U. Bandelow. *Theorie longitudinaler Effekte in 1.55 μm Mehrsektions DFB-Laserdioden*. PhD thesis, Humboldt-Universität Berlin, 1994.
- [2] U. Bandelow, L. Recke and B. Sandstede. Frequency regions for forced locking of self-pulsating multi-section DFB lasers. *Opt. Comm.*, **147**, 212–218, 1998.
- [3] U. Bandelow, M. Wolfrum, M. Radziunas and J. Sieber. Impact of gain dispersion on the spatio-temporal dynamics of multisection lasers. *IEEE J. of Quant El.*, **37**(2), 183–189, 2001.
- [4] P. W. Bates, K. Lu and C. Zeng. Existence and persistence of invariant manifolds for semiflows in Banach spaces. *Mem. Amer. Math. Soc.*, **135**, 1998.
- [5] P. W. Bates, K. Lu and C. Zeng. Persistence of overflowing manifolds for semiflow. *Comm. Pure Appl. Math.*, **52**(8), 983 – 1046, 1999.
- [6] P. W. Bates, K. Lu and C. Zeng. Invariant foliations near normally hyperbolic invariant manifolds for semiflows. *Trans. Amer. Math. Soc.*, **352**, 4641–4676, 2000.
- [7] S. Bauer, O. Brox, J. Kreissl, B. Sartorius, M. Radziunas, J. Sieber, H.-J. Wünsche and F. Henneberger. Nonlinear dynamics of semiconductor lasers with active optical feedback. *Phys. Rev. E*, **69**, 016206, 2004.
- [8] O. Brox, S. Bauer, M. Radziunas, M. Wolfrum, J. Sieber, J. Kreissl, B. Sartorius and H.-J. Wünsche. High-frequency pulsations in DFB-lasers with amplified feedback. *IEEE J. Quantum Elect.*, **39**(11), 1381 – 1387, 2003.
- [9] O. Diekmann, S. van Gils, S. M. Verduyn Lunel and H.-O. Walther. *Delay Equations*, volume 110 of *Applied Mathematical Sciences*. Springer-Verlag, 1995.
- [10] E. J. Doedel, A. R. Champneys, T. F. Fairgrieve, Y. A. Kuznetsov, B. Sandstede and X. Wang. *AUTO97, Continuation and bifurcation software for ordinary differential equations*, 1998.
- [11] N. Fenichel. Geometric singular perturbation theory for ordinary differential equations. *Journal of Differential Equations*, **31**, 53–98, 1979.
- [12] S. Friese. Existenz und Stabilität von Lösungen eines Randanfangswertproblems der Halbleiterdynamik. Master's thesis, Humboldt-Universität Berlin, 1999.
- [13] F. Jochmann and L. Recke. Existence and uniqueness of weak solutions of an initial boundary value problem arising in laser dynamics. Preprint 515, WIAS, 1999.
- [14] B. Krauskopf, K. Schneider, J. Sieber, S. Wieczorek and M. Wolfrum. Excitability and self-pulsations near homoclinic bifurcations in laser systems. *Opt. Comm.*, **215**, 367–379, 2003.
- [15] D. Marcenac. *Fundamentals of laser modelling*. PhD thesis, University of Cambridge, 1993.
- [16] M. Möhrle, B. Sartorius, C. Bornholdt, S. Bauer, O. Brox, A. Sigmund, R. Steingrüber, M. Radziunas and H.-J. Wünsche. Detuned grating multisection-RW-DFB lasers for high speed optical signal processing. *IEEE J. on Sel. Top. Quantum Electron.*, **7**, 217–223, 2001.

- [17] A. Pazy. *Semigroups of Linear Operators and Applications to Partial Differential Equations*. Applied mathematical Sciences. Springer Verlag, New York, 1983.
- [18] D. Peterhof and B. Sandstede. All-optical clock recovery using multisection distributed-feedback lasers. *J. Nonlinear Sci.*, **9**, 575–613, 1999.
- [19] M. Radziunas, H.-J. Wünsche, B. Sartorius, O. Brox, D. Hoffmann, K. Schneider and D. Marcenac. Modeling self-pulsating DFB lasers with integrated phase tuning section. *IEEE J. of Quant. El.*, **36**(9), 1026–1034, 2000.
- [20] L. Recke, K.R. Schneider and V.V. Strygin. Spectral properties of coupled wave equations. *Z. angew. Math. Phys.*, **50**, 923–933, 1999.
- [21] J. Sieber. Numerical bifurcation analysis for multi-section semiconductor lasers. *SIAM J. of Appl. Dyn. Sys.*, **1**(2), 248–270, 2002.
- [22] J. Sieber. Longtime behavior of the coupled traveling wave model for semiconductor lasers. Preprint 23, University of Bristol, Dept. of Eng. Math., 2003.
- [23] B. Tromborg, H. E. Lassen and H. Olesen. Travelling wave analysis of semiconductor lasers. *IEEE J. of Quant. El.*, **30**(5), 939–956, 1994.
- [24] D. Turaev. Fundamental obstacles to self-pulsations in low-intensity lasers. Preprint 629, WIAS, 2001. Submitted to SIAM J. of Appl. Math
- [25] H. Wenzel, U. Bandelow, H.-J. Wünsche and J. Rehberg. Mechanisms of fast self pulsations in two-section DFB lasers. *IEEE J. of Quant. El.*, **32**(1), 69–79, 1996.
- [26] M. Wolfrum and D. Turaev. Instabilities of lasers with moderately delayed optical feedback. *Opt. Comm.*, **212**(1-3), 127 – 138, 2002.
- [27] H. J. Wünsche, O. Brox, M. Radziunas and F. Henneberger. Excitability of a semiconductor laser by a two-mode homoclinic bifurcation. *Phys. Rev. Lett.*, **88**(2), 023901, 2002.
- [28] H.-J. Wünsche, M. Radziunas, S. Bauer, O. Brox and B. Sartorius. Simulation of phase-controlled mode-beating lasers. *IEEE J. Selected Topics of Quantum Electron*, **9**(3), 857 – 864, 2003.

Daugiasekcijinių puslaidininkinių lazerių dinamika

J. Sieber, M. Radžiūnas, K.R. Schneider

Mes nagrinėjame išilginę daugiasekcijinių puslaidininkinių lazerių dinamiką, kuri yra nusakoma netiesiškai susietomis hiperboline diferencialinių lygčių dalinėmis išvestinėmis bei paprastujų diferencialinių lygčių sistemomis. Mes pateikiame sekantias šios sistemos savybes: globalaus pradinio-kraštiniuo uždavinio sprendinio egzistavimas bei vienatis; mažos dimensijos pritraukiančiojo invariantinio hiperpaviršiaus egzistavimas. Modelio dinamika šiame hiperpaviršiuje yra apytiksliai nusakoma paprastujų diferencialinių lygčių sistema. Pabaigoje mes pateikiame detalią skaitinę šios paprastujų diferencialinių lygčių sistemos bifurkacinių analizę ir lyginame ją su skaitiškai nustatyta pilnos diferencialinių lygčių dalinėmis išvestinėmis sistemos dinamika.